Symmetry Method for the Absolute Determination of Energy-Band Dispersions $E(k)$ Using Angle-Resolved Photoelectron Spectroscopy

Eberhard Dietz[a] and D. E. Eastman
IBM Thomas J. Watson Research Center, Yorktown Heights, New York 10598
(Received 8 August 1978)

Angle-resolved spectra for emission in a mirror plane as a function of emission angle and photon energy $h\nu$ show critical-point behavior in interband intensities for transitions on zone boundaries. For such transitions, the absolute energies E and crystal momentum $\vec{k}$ for both the initial and final states are given by $h\nu$ and the emission angle. $E(\vec{k})$ dispersions have been determined for several d bands and conduction bands along the Δ, Λ, and Σ axes of copper.

Energy-band dispersions $E(\vec{k})$ are of fundamental interest since they are the basic quantity in the one-electron picture of solids upon which much of our physical understanding of condensed matter rests. Angle-resolved photoelectron spectroscopy (ARPES) is an outstanding tool for determining $E(\vec{k})$ dispersions for surfaces and solids.[1-4] For "two-dimensional" bands (e.g., surface bands) $E(\vec{k}_t)$ dispersions, where $\vec{k}_t$ is the wave vector parallel to the surface, are directly obtained by measuring the electron kinetic energy $E_{\rm kin}$ and emission angle. For solids, however, the momentum component normal to the surface ($\vec{k}_n = \vec{k} - \vec{k}_t$) must also be determined; $\vec{k}_n$ changes during the emission process and cannot be directly measured. The $E(\vec{k})$ dispersions for interband transitions can be determined only insofar as $\vec{k}_n$ of either the initial or the final Bloch state can be deduced.

Most experiments on $E(\vec{k})$ dispersions over a finite energy and momentum range have been done with normal emission from low-index planes of single crystals.[4] By use of some assumption for one of the states involved (e.g., a calculated E vs $\vec{k}_n$ for the final state[3]), $E(\vec{k})$ dispersions can be determined for various bands along symmetry lines normal to the surface. Off-normal ARPES together with parametrized band models[5] have been used to probe $E(\vec{k})$ dispersions along arbitrary lines in $\vec{k}$ space, yielding the $E(\vec{k})$ along symmetry lines indirectly.[1,2,6] In principle, unknown $\vec{k}_n$ can be determined by comparison of angular-dependent structures in appropriate spectra from two different crystal faces[7]; however, applications of this method have been limited.[8]

In this paper we describe a new method for the absolute determination of $E(\vec{k})$ band dispersions along symmetry lines using off-normal ARPES with tunable synchrotron radiation. The only assumption required in interpreting the experiments is that the general $E(\vec{k})$ topology of the conduction bands be relatively simple or qualitatively known,[9] i.e., similar to that given by the usual band calculations.[10,11] $E(\vec{k})$ dispersions have been determined for several valence and conduction bands along the Δ, Λ, and Σ axes for copper up to 25 eV above the Fermi level $E_{\rm F}$, including bands which cannot be probed in normal emission experiments because of vanishing matrix elements.[12,13]

Angle-resolved energy-distribution curves (AREDC's) have been measured for a single-crystal Cu(111) surface using a modified cylindrical mirror analyzer[14] and synchrotron radiation at the Physical Sciences Laboratory at the University of Wisconsin–Madison. An angular resolution of $\delta\Omega = 4°$ (full angle) and a typical total energy resolution of 0.15 eV were attained; the AREDC's were normalized to constant photon flux by use of a sodium salicylate detector as a reference.[15] AREDC's were measured with emission in the $(1\bar{1}0)$ mirror plane for polar angles in the range of $-60° \leq \vartheta \leq +60°$ and for photon energies in the range $10 \leq h\nu \leq 30$ eV. For most AREDC's, the polarization of the incident radiation was selected to be perpendicular to the $(1\bar{1}0)$ mirror plane of detection ($\hat{a} \| [1\bar{1}0]$).

Figure 1 shows a series of $h\nu$-dependent AREDC's obtained for a fixed angle of detection ($\vartheta = -30°$). As given by symmetry rules for dipole matrix elements[12,13] and our polarization, the AREDC's for Cu are dominated by two main peaks[16] due to the two initial states of odd parity with respect to the $(1\bar{1}0)$ mirror plane.[1,2] A striking feature in these AREDC's is the qualitative spectral change as the photon energy $h\nu$ increases from 14 to 15 eV; i.e., a peak with $E_i = -3.1$ eV binding energy suddenly appears while the peak with $E_i = -2.8$ eV decreases in intensity by $\sim\frac{1}{2}$. Similarly, for $h\nu \geq 26$ eV the peak at $E_i = -3.6$ eV suddenly decreases in intensity to $\sim\frac{1}{6}$ of its height. As will be described using Fig. 2, both of these features occur when the final-state transitions cross zone boundaries in the extended-

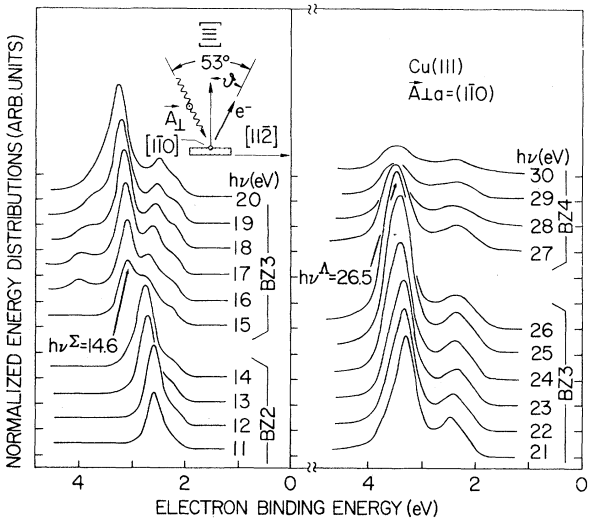

FIG. 1. Normalized angle-resolved energy-distribution curves (AREDC's) for a fixed direction of observation, $\vartheta = -30°$, in the $(1\bar{1}0)$ plane. With variation of the photon energy $h\nu$, the final-state transitions occur in different Brillouin zones as marked. The strong changes in peak height are due to zone-boundary crossings.

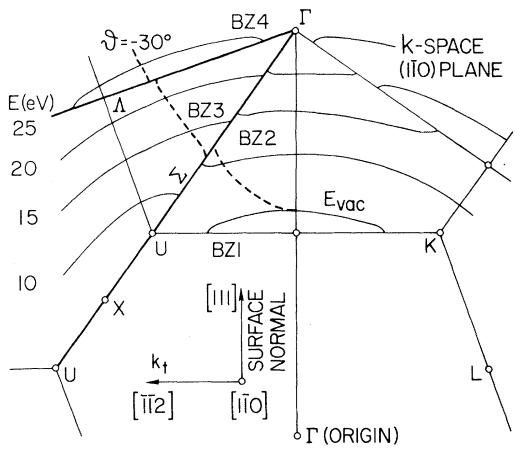

FIG. 2. Cut through the extended-zone scheme of a fcc metal. The different Brillouin-zone segments are marked by BZ1 to BZ4. The solid lines are the contours of constant energy for nearly-free-electron-like final states and are essentially circles about the origin with distortions due to the band gaps at zone boundaries. The dashed line is the locus of final states which can contribute to specular emission into the $\vartheta = -30°$ direction, i.e., where all direct transitions observed in Fig. 1 origniate, independent of their particular energy.

zone scheme.

Figure 2 is a momentum-space plot of the $(1\bar{1}0)$ mirror plane in the extended-zone scheme. Conservation of $\vec{k}_t$ provides that all electrons emitted in the $(1\bar{1}0)$ plane as a result of direct transitions arise from final states in this plane. Portions of the first through fourth Brillouin zones (BZ1 through BZ4) for the fcc lattice and their boundaries (straight lines) are outlined. The boundaries between BZ2 and BZ3 and between BZ3 and BZ4 are the Σ and Λ axes, respectively (heavy lines). Also given in Fig. 2 is a schematic sketch of the nearly-free-electron-like final-state energy bands. Thus, in the extended-zone scheme, the contours of constant final energy are circles about the origin Γ, with deviations near zone boundaries due to the usual symmetry gaps. Each energy contour in BZ2 and BZ3 that intersects on the Σ axis terminates at two different points corresponding to two points on the Σ_3 and Σ_1 lines in the conventional $E(\vec{k})$ band structure plots.

The dashed line in Fig. 2 is the locus of final states which can contribute to specular emission into the $\vartheta = -30°$ direction. Thus, direct transitions observed in Fig. 1—independent of their particular energy—all originate on this line in momentum space. This locus is given by the conditions for conservation of energy and momentum for electron emission through a smooth surface: $E_{\rm kin} = E - E_{\rm vac}$ is the vacuum level, and $\vec{k}_t' = \vec{k}_t + G_0$, where $\vec{k}_t'$ is the measured momentum of the electron in free space parallel to the surface and $\vec{G}_0$ is a reciprocal surface lattice vector. For emission without surface umklapp processes[17] (i.e., $\vec{G}_0 = 0$) this condition can be rewritten as

$$\vec{k}_t = \vec{e}(2mE_{\rm kin})^{1/2}\hbar^{-1}\sin\vartheta, \qquad (1)$$

where the unit vector $\vec{e}$ points in the $[11\bar{2}]$ direction. The specific position of the observed transitions (Fig. 1) on the locus $\vartheta = \text{const}$ is implicitly given by $E(\vec{k}) - E_i(\vec{k}) = h\nu$ and is unknown in general since the dispersion $E(\vec{k})$ is not known. However, starting at low photon energies just above threshold, the transitions can only occur into final states in BZ2. With increasing $h\nu$, the wave vector for emission at $\vartheta = 30°$ moves upwards along the dashed line of Fig. 2 and crosses the boundary into BZ3 [i.e., crosses the Σ line in the $(1\bar{1}0)$ plane for some photon energy, which we experimentally find to be $h\nu_0 = 14.6$ eV]. Upon crossing the zone boundary the wave-function character of the states change rapidly with $\vec{k}$, thus providing strong variations of transition ma-

trix elements[18] and giving rise to the observed $h\nu$-dependent behavior shown in Fig. 1. Similarly, crossing the Λ axis from BZ3 into BZ4 causes a drop of peak intensity for $h\nu > 26.5$ eV.

Energy dispersions $E(\vec{k})$ are directly obtained as follows. The initial-state eigenvalue E_i for the $\vec{k}$ point where the locus $\vartheta = -30°$ reaches the symmetry axis can directly be obtained for a given peak from the AREDC corresponding to its "critical" photon energy. The final-state energy follows from the relation $E = E_i + h\nu$. Changing ϑ and applying the same procedure gives the eigenvalues for other $\vec{k}$ points along the Σ and Λ axes. The connection to the conventional plotting of $E(\vec{k})$ along symmetry lines is given in Fig. 3. The series of dashed lines give the loci of possible values of E vs $\vec{k}$ along the Λ, Δ, and Σ symmetry lines which may be obtained for emission in the denoted ϑ directions and the dots give our experimental values. The E-vs-$\vec{k}$ relation for ϑ fixed is given by $E = E_{\text{vac}} + (\hbar k)^2/(2m\cos^2\alpha \sin^2\vartheta)$, where k is the value on the symmetry line measured from Γ and $\cos\alpha$ is the direction cosine between $\vec{k}_i$ and the symmetry axis under consideration (i.e., $\alpha = 54.7°$, $19.5°$, and $35.3°$ for the Σ, Λ, and Δ symmetry axes, respectively.

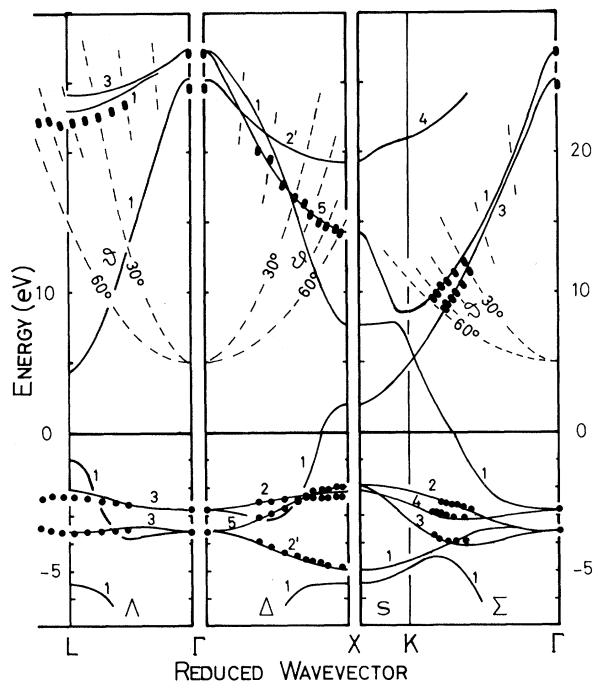

FIG. 3. Experimental E-vs-$\vec{k}$ band structure of Cu (dots). For each denoted direction, the dashed line gives the E-vs-$\vec{k}$ loci on the symmetry axis for which emissions may be obtained (see text). For comparison, the solid lines represent the calculated band structure of Ref. 11.

The final-state error bounds are due to electron lifetime broadening (see below) while the initial d-state error bounds are mainly due to the uncertainty of the position of the transition along the axis. For $0 < |\vartheta| \leq 20°$, no data are given because the analysis is complicated by the occurrence of several closely spaced zone boundaries near Γ. For normal emission from the (111) surface, strong $h\nu$-dependent peak-intensity variations have been observed and analyzed with the same method. States along the Δ_2 and Σ_3 lines have been determined using mixed polarized light.

In our evaluation of $E(\vec{k})$ points, the broadening Γ as well as $h\nu$-dependent matrix elements $|M_{if}|^2$ have been considered. "Critical" photon energies $h\nu_0$ are found by fitting the observed peak heights $F(\nu_n)$ at discrete $h\nu_n$'s within $\sim 2\Gamma$ of $h\nu_0$ with the expression

$$F(\nu_n) = C \int_{\nu_0 - 3\Gamma}^{\nu_0 + 3\Gamma} |M_{if}(\nu)|^2 \times \frac{\Gamma^2}{(h\nu - h\nu_n)^2 + \Gamma^2} d\nu, \qquad (2)$$

where Γ (full width at half maximum) for $\vartheta = -30°$ is estimated to be $\Gamma/E \simeq \delta(h\nu)/h\nu \simeq 5\%$ and 8% near the Σ and Λ axes, respectively.[19] The functional dependence of $|M_{if}(\nu)|^2$—which we have assumed to be a linear function near the zone boundary within each BZ—and $h\nu_0$ are optimized, thus determining $h\nu_0$ and consequently the AREDC from which the final- and initial-state energies and the momentum $\vec{k}$ are found.

The solid lines in Fig. 3 depict the self-consistent Korringa-Kohn-Rostoker band calculation of Janak, Williams, and Moruzzi.[11] The agreement for both the initial and final states is good. Because the error bounds (due to electron lifetime broadening and our crude treatment of the $h\nu$-dependent matrix elements) are fairly large, an accurate test of the calculated $E(\vec{k})$ dispersions at high energies is difficult. However, there is some indication that for $E > 20$ eV the self-energy correction of Ref. 11 has to be reduced.

We acknowledge the able assistance of the Physical Sciences Laboratory staff and thank Ulrich Gerhardt, F. J. Himpsel, J. A. Knapp, and N. V. Smith for helpful discussions. The project was supported in part by the Sonderforschungsbereich 65 "Festkörperspektroskopie" Darmstadt/Frankfurt and by the U. S. Air Force Office of Scientific Research under Contract No. F44620-76-C-

0041.

[a]Permanent address: Physikalisches Institut der Universitaet Frankfurt, D-6000 Frankfurt am Main 1, West Germany.

[1]E. Dietz, H. Becker, and U. Gerhardt, Phys. Rev. Lett. 36, 1397 (1976), and 37, 115 (1976).

[2]Eberhard Dietz and Ulrich Gerhardt, to be published.

[3]J. A. Knapp, F. J. Himpsel, and D. E. Eastman, to be published.

[4]For a recent bibliography, see Ref. 3.

[5]N. V. Smith and L. F. Mattheiss, Phys. Rev. B 9, 1341 (1974), and references therein.

[6]L. Ilver and P. O. Nilsson, Solid State Commun. 18, 677 (1976).

[7]E. O. Kane, Phys. Rev. Lett. 12, 97 (1964).

[8]R. R. Turtle and T. A. Callcott, Phys. Rev. Lett. 34, 86 (1975).

[9]This method is generally useful for metals, but its application to semiconductors, which have more complicated conduction bands, has not yet been explored.

[10]G. A. Burdick, Phys. Rev. 129, 138 (1963).

[11]J. F. Janak, A. R. Williams, and V. L. Moruzzi, Phys. Rev. B 11, 1522 (1975); the "self-energy" correction of $\lambda = 0.08$ is included. The $E(\vec{k})$ for the Σ axis has been provided by private communication.

[12]G. W. Gobeli, F. G. Allen, and E. O. Kane, Phys. Rev. Lett. 12, 94 (1964).

[13]J. Hermanson, Solid State Commun. 22, 9 (1977).

[14]J. A. Knapp, G. J. Lapeyre, N. V. Smith, and M. M. Traum, to be published.

[15]J. A. R. Samson, *Vacuum Ultraviolet Spectroscopy* (Wiley, New York, 1967), p. 212.

[16]The shoulder at $E_i \simeq -2.2$ eV is assigned to surface umklapp emission and will not be treated in this paper.

[17]G. D. Mahan, Phys. Rev. B 2, 4334 (1970).

[18]The transition matrix element is expected to exhibit an asymmetric behavior upon crossing a zone boundary since the reduced $\vec{k}$ vector of the periodic initial state changes sign whereas the momentum of the free-electron-like final state continues smoothly across the boundary.

[19]D. E. Eastman, J. A. Knapp, and F. J. Himpsel, Phys. Rev. Lett. 41, 825 (1978). Although the final state is broadened, sharp peaks are observed because the dispersion of the initial states is small.

Experimental Determination of the Density Dependence of Electron-Hole Correlation in Electron-Hole Liquid

H.-h. Chou and George K. Wong

Physics Department and Materials Research Center, Northwestern University, Evanston, Illinois 60201

(Received 30 March 1978)

We report measurements of total lifetime and e-h pair density of electron-hole liquid in Ge under ⟨111⟩ uniaxial stress. We show that the density dependence of electron-hole correlation can be estimated semiquantitatively from our data. Our result gives the first experimental evidence that electron-hole correlation increases rapidly as the e-h pair density is lowered. We compare our results with calculations based on different many-body theoretical approximations.

The discovery of electron-hole droplets (EHD) in semiconductors has prompted several many-body calculations of the ground-state properties of this unique quantum liquid system.[1-3] The ground-state energies and densities obtained from these calculations are in reasonable agreement with each other and with experimental results. These calculations, however, make significantly different predictions of electron-hole correlation as measured by the enhancement factor $g_{eh}(0)$, which denotes the value of the e-h pair correlation function $g_{eh}(r)$ for zero interparticle separation. The more sophisticated calculation[3] based on a self-consistent theory of Singwi *et al.*[4] (STLS) predicts a much larger value of $g_{eh}(0)$ than that given by using either the Hubbard or the RPA approximation.[2,3] The discrepancy becomes even greater as the density is lowered. Since the enhancement factor is a direct measure of the wave function, it provides a more sensitive test of the theoretical approximations than does the calculation of the ground-state energy. In principle, the enhancement factor can be determined experimentally by comparing the measured radiative decay rate of e-h pairs in EHD with that measured for exciton[5] or uncorrelated plasma.[6] However, it is difficult to obtain unambiguously an absolute value of the enhancement factor using these two methods. This has, hitherto, prevented any meaningful comparison between theory and experiment as regards $g_{eh}(0)$. Such a comparison would be very valuable in that

